A&A, 707, C3 (2026)
https://doi.org/10.1051/0004-6361/202659479e

Astronomy & Astrophysics

Investigating chemical variations between interstellar gas clouds in the solar neighbourhood *(Corrigendum)*

T. Ramburuth-Hurt[1,⋆], A. De Cia[1,2], J.-K. Krogager[3,4], C. Ledoux[5], E. Jenkins[6], A. J. Fox[7,8], C. Konstantopoulou[1], A. Velichko[1,9], and L. Dalla Pola[1]

[1] Department of Astronomy, University of Geneva, Chemin Pegasi 51, Versoix, Switzerland
[2] European Southern Observatory, Karl-Schwarzschild-Str. 2, 85748 Garching, Germany
[3] Université Claude Bernard Lyon 1, Centre de Recherche Astrophysique de Lyon UMR5574, 9 Av. Charles André, 69230 Saint-Genis-Laval, France
[4] French-Chilean Laboratory for Astronomy (FCLA), CNRS-IRL3386, U. de Chile, Camino el Observatorio 1515, Casilla 36-D, Santiago, Chile
[5] European Southern Observatory, Alonso de Córdova 3107, Vitacura, Casilla 19001, Santiago, Chile
[6] Department of Astrophysical Sciences, Princeton University, Princeton, NJ 08544-1001, USA
[7] AURA for ESA, Space Telescope Science Institute, 3700 San Martin Drive, Baltimore, MD 21218, USA
[8] Department of Physics & Astronomy, Johns Hopkins University, 3400 N. Charles Street, Baltimore, MD 21218, USA
[9] Institute of Astronomy, Kharkiv National University, 4 Svobody Sq., Kharkiv 61022, Ukraine

A&A, 695, A14 (2025), https://doi.org/10.1051/0004-6361/202451729

Key words. Galaxy: abundances – Galaxy: general – local insterstellar matter – solar neighborhood – errata, addenda

We have identified a mistake in the calculation of the total hydrogen column densities for all eight lines of sight in this sample. In the text of the paper, we report the total hydrogen as $N(\mathrm{H_{tot}}) = N(\mathrm{H\,I}) + \times N(\mathrm{H_2})$. However, it should be $N(\mathrm{H_{tot}}) = N(\mathrm{H\,I}) + 2N(\mathrm{H_2})$, with the factor of 2 on $N(\mathrm{H_2})$. The effect of this is a slight decrease in metallicities, both for the full line-of-sight measurements, $[\mathrm{M/H}]_{\mathrm{tot}}$, $[\mathrm{M/H}]_{\mathrm{ref}}$, and $[\mathrm{M/H}]_{\mathrm{vol}}$, and the simulations of metallicities of individual gas clouds, $[\mathrm{M/H}]_i$. The only unaffected line of sight is that towards θ^1 Ori C because it has a negligible contribution from $\mathrm{H_2}$. The methodology of the paper remains unaffected, as do all measurements of dust depletion, for both the full line of sight, $[\mathrm{Zn/Fe}]_{\mathrm{fit,\,tot}}$, and individual (groups of) components, $[\mathrm{Zn/Fe}]_{\mathrm{fit},\,i}$. The levels of variations in the metallicities from the simulations also do not change. Therefore, the overall conclusions of the paper remain valid. We still constrain the same metallicities, but these values are slightly lower than presented in the paper. In summary, the consequences are the following:

- The total metallicities along full lines of sight are generally lower, with changes between 0.08 and 0.16 dex, or 17% and 31%.
- This decreases the values of the simulated metallicities by the same margin.
- This increases the number of 'most-likely' realisations because there are many more realisations with all metallicities <0.5 dex.
- This broadens the gas fraction ranges for all 'most-likely' realisations.

In Table 1, we show the updated values and quantify the differences, in terms of both a percentage and dex increase. We reproduce Tables 5, 6, 7, and 8 from the paper for the impacted lines of sight in Tables 2, 3, 5, and 4, respectively. In Appendices A and B, we include the updated figures for the abundance patterns and simulated metallicities, respectively. In Appendix C we include the comparison-to-literature plot with the updated metallicity values for the full lines of sight.

We have also noticed that Fig. 7 in the original paper, which shows the realisations of the most-likely metallicities for the line of sight towards θ^1 Ori C, is not accurate. Figure 1 here is the corrected version.

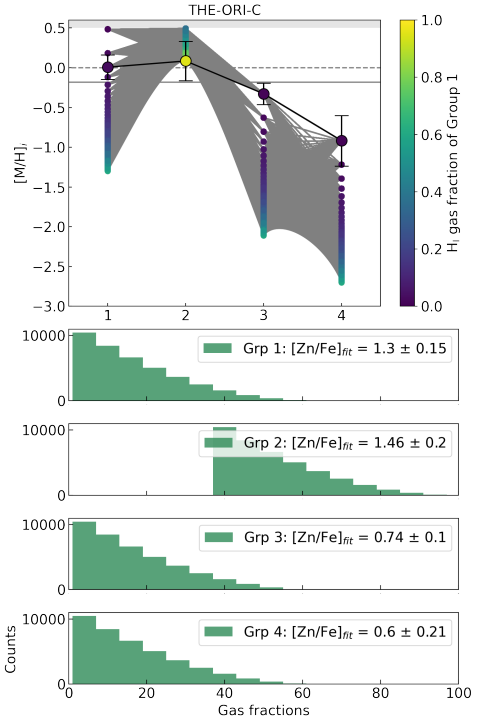

Fig. 1. Corrected version of Fig. 6 from the original paper.

⋆ Corresponding author: tanita.ramburuth-hurt@unige.ch

Table 1. Updated hydrogen column densities.

Target	$\log N(\mathrm{H\,I})$	$\log N(\mathrm{H_2})$	$\log N(\mathrm{H\,I} + \mathrm{H_2})$	$\log N(\mathrm{H\,I} + 2 \times \mathrm{H_2})$	Increase %	Increase dex
θ^1 Ori C	21.59 ± 0.03	17.25 ± 0.10	21.59 ± 0.10	21.59 ± 0.03	0	0
HD 110432	21.03 ± 0.03	20.64 ± 0.10	21.18 ± 0.10	21.29 ± 0.05	29	0.11
ρ Oph A	21.63 ± 0.03	20.57 ± 0.10	21.67 ± 0.10	21.70 ± 0.03	8	0.03
χ Oph	21.21 ± 0.03	20.63 ± 0.10	21.31 ± 0.10	21.39 ± 0.04	21	0.08
HD 154368	21.27 ± 0.05	21.16 ± 0.10	21.52 ± 0.11	21.68 ± 0.06	44	0.16
κ Aql	20.94 ± 0.03	20.31 ± 0.10	21.03 ± 0.10	21.11 ± 0.04	19	0.08
HD 206267	21.24 ± 0.04	20.86 ± 0.10	21.39 ± 0.11	21.50 ± 0.05	29	0.11
HD 207198	21.28 ± 0.04	20.83 ± 0.10	21.41 ± 0.11	21.51 ± 0.05	26	0.10

Table 2. Five sight lines where the component with the highest depletion also contains the majority of the hydrogen gas.

Target	Group	$[\mathrm{Zn/Fe}]_{\mathrm{fit,i}}$	f_i	$[\mathrm{M/H}]_i \geq$
χ Oph	3	2.03 ± 0.13	$45\% < f_3 < 90\%$	0.19 ± 0.16
HD 154368	4	1.85 ± 0.09	$27\% < f_4 < 93\%$	−0.05 ± 0.16
κ Aql	2	1.74 ± 0.09	$36\% < f_2 < 87\%$	0.11 ± 0.13
HD 207198	2	1.55 ± 0.14	$31\% < f_2 < 82\%$	0.06 ± 0.22

Table 3. Metallicities and corresponding gas fractions for the cases with the minimum difference in metallicity.

Target	Group	$[\mathrm{M/H}]_i$	f_i (%)
HD 110432	1	0.26 ± 0.78	4
	2	0.30 ± 0.12	96
χ Oph	1	0.28 ± 0.16	2
	2	0.23 ± 0.08	12
	3	0.22 ± 0.19	84
	4	0.19 ± 0.22	2
HD 154368	1	0.07 ± 0.14	5
	2	−0.01 ± 0.29	4
	3	0.03 ± 0.31	3
	4	−0.01 ± 0.16	86
	5	0.06 ± 0.41	2
κ-Aql	1	0.20 ± 0.15	2
	2	0.17 ± 0.14	76
	3	0.15 ± 0.10	20
	4	0.21 ± 0.38	1
	5	0.22 ± 0.11	1
HD 206267	1	−0.24 ± 0.18	6
	2	−0.22 ± 0.12	94
HD 207198	1	0.18 ± 0.26	35
	2	0.18 ± 0.22	61
	3	0.20 ± 0.73	4

Table 4. Minimum and maximum metallicities and their respective *z*-test significance for the minimum-difference realisation.

Target	Min. $[\mathrm{M/H}]_i$	Max. $[\mathrm{M/H}]_i$	Diff. (dex)	*z-test* (σ)
HD 110432	0.26 ± 0.78	0.30 ± 0.12	0.04	0
χ Oph	0.19 ± 0.16	0.28 ± 0.16	0.10	0.4
HD 154368	–0.01 ± 0.16	0.07 ± 0.14	0.08	0.2
κ Aql	0.15 ± 0.10	0.22 ± 0.11	0.07	0.5
HD 206267	−0.24 ± 0.18	−0.22 ± 0.12	0.02	0.1
HD 207198	0.18 ± 0.22	0.20 ± 0.73	0.02	0

Notes. The results for θ^1 Ori C are in the original paper.

Table 5. Results from the abundance patterns for each target along the full line of sight.

Target	No. comps	Groups of comps	$[\mathrm{M/H}]_{\mathrm{tot}}$	$[\mathrm{Zn/Fe}]_{\mathrm{fit,tot}}$	$[\mathrm{M/H}]_{\mathrm{ref}}$	$[\mathrm{M/H}]_{\mathrm{vol}}$	$[\mathrm{M/H}]_{\mathrm{DC21}}$	$[\mathrm{M/H}]_{\mathrm{R23}}$ All metals
θ^1 Ori C	16	4	0.06 ± 0.20	1.46 ± 0.20	–	0.20 ± 0.10	−0.50 ± 0.20	–
HD 110432	6	2	0.26 ± 0.07	1.78 ± 0.06	0.11 ± 0.27	[0.32]	−0.14 ± 0.15	
ρ Oph A	15	2	[0.33]	[1.91]	–	–	−0.78 ± 0.12	−0.036 ± 0.094
χ Oph	19	4	0.04 ± 0.05	1.66 ± 0.06	0.02 ± 0.19	0.23 ± 0.06	−0.33 ± 0.11	–
HD 154368	11	5	−0.16 ± 0.08	1.45 ± 0.08	−0.60 ± 0.2	−0.18 ± 0.21	−0.42 ± 0.12	
κ Aql	16	5	0.14 ± 0.09	1.60 ± 0.07	−0.22 ± 0.2	0.31 ± 0.18	−0.22 ± 0.14	
HD 206267	7	2	0.05 ± 0.14	1.51 ± 0.12	−0.66 ± 0.3	0.32 ± 0.31	−0.21 ± 0.12	−0.097 ± 0.067
HD 207198	6	2	0.16 ± 0.14	1.56 ± 0.12	−0.76 ± 0.13	0.42 ± 0.21	−0.67 ± 0.08	−0.05 ± 0.067

Appendix A: Updated abundance pattern figures

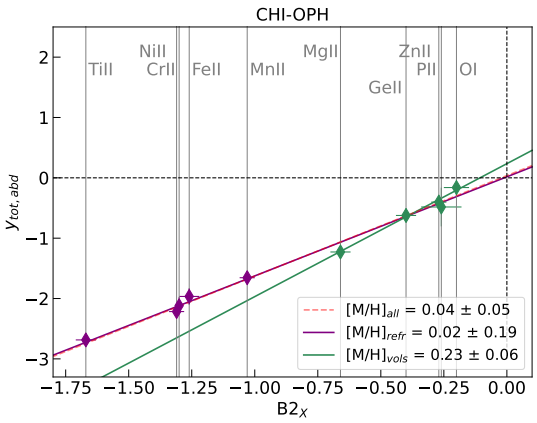

Fig. A.1: Updated abundance pattern for χ Oph.

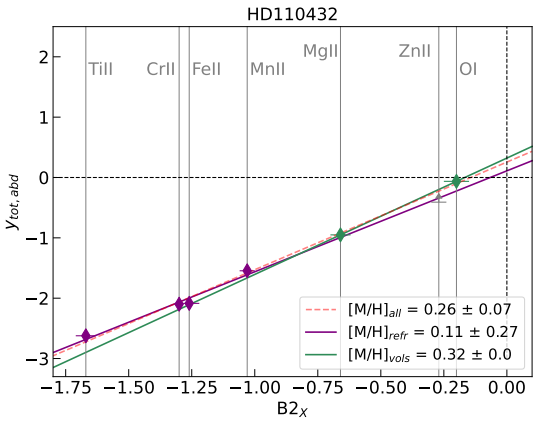

Fig. A.2: Updated abundance pattern for HD 110432.

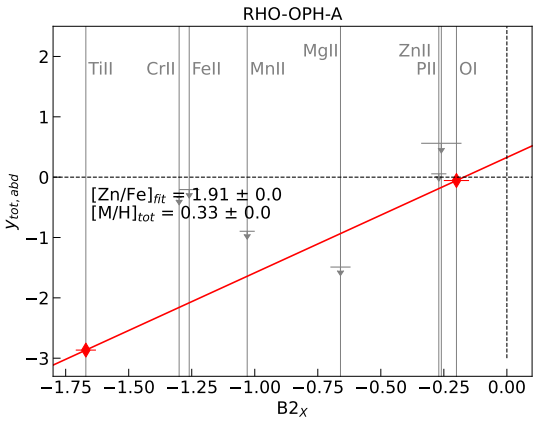

Fig. A.3: Updated abundance pattern for ρ Oph A.

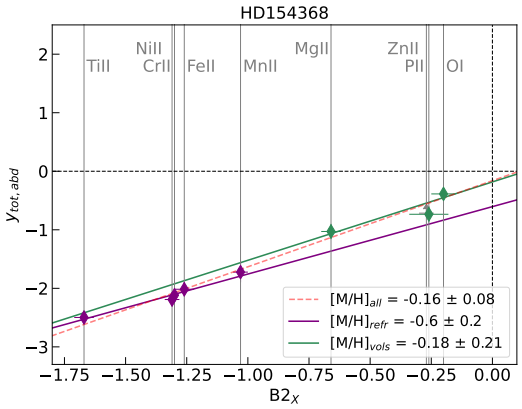

Fig. A.4: Updated abundance pattern for HD 154368.

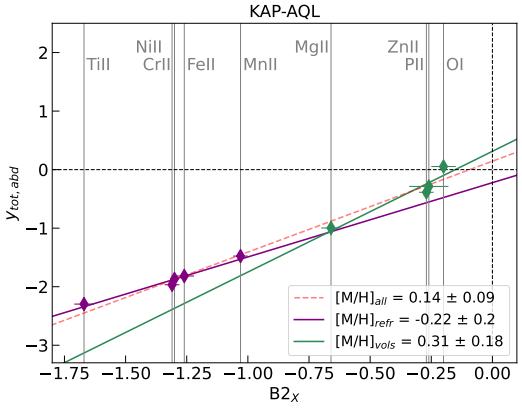

Fig. A.5: Updated abundance pattern for κ Aql.

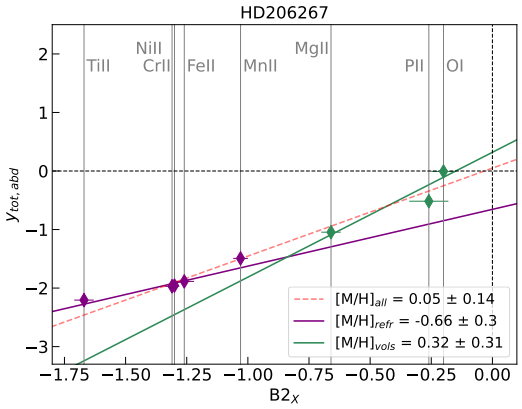

Fig. A.6: Updated abundance pattern for HD 206267.

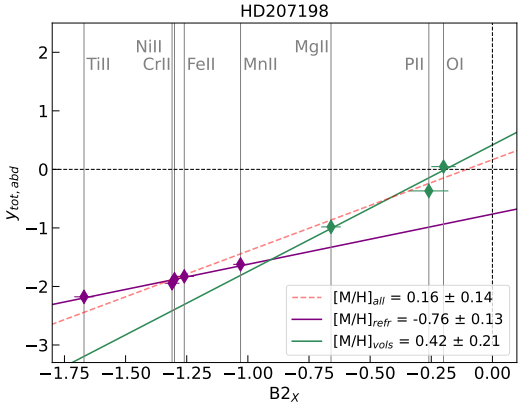

Fig. A.7: Updated abundance pattern for HD 207198.

Appendix B: Updated simulated metallicity figures

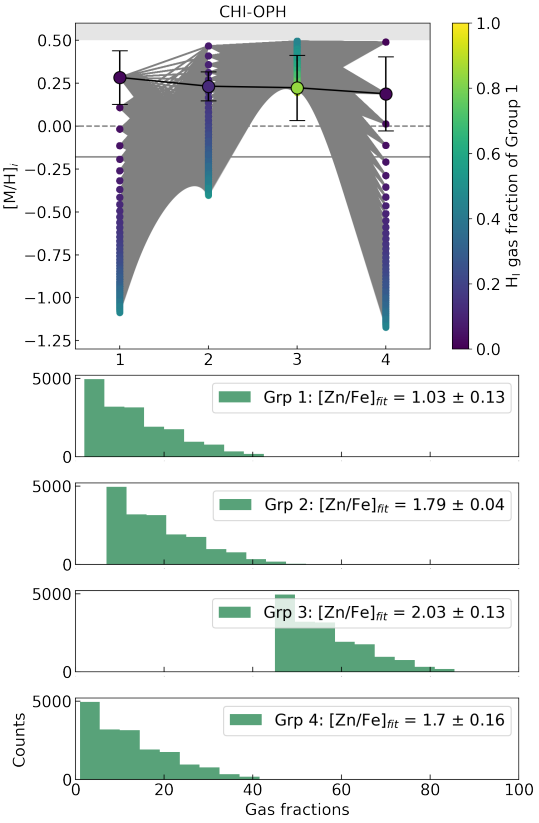

Fig. B.1: Updated simulated metallicities for χ Oph.

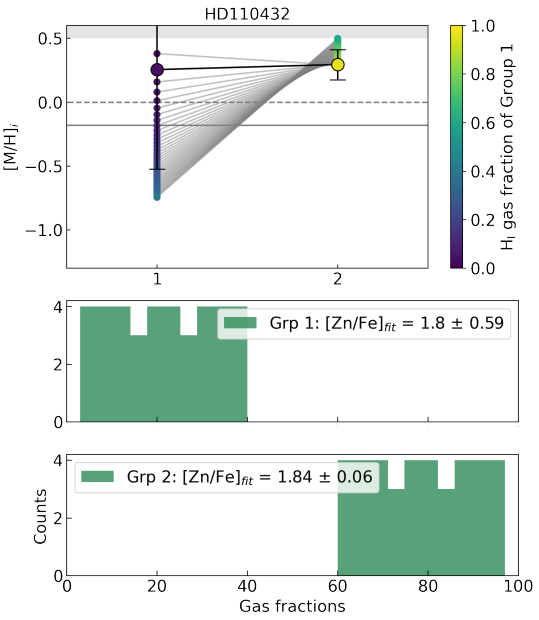

Fig. B.2: Updated simulated metallicities for HD 110432.

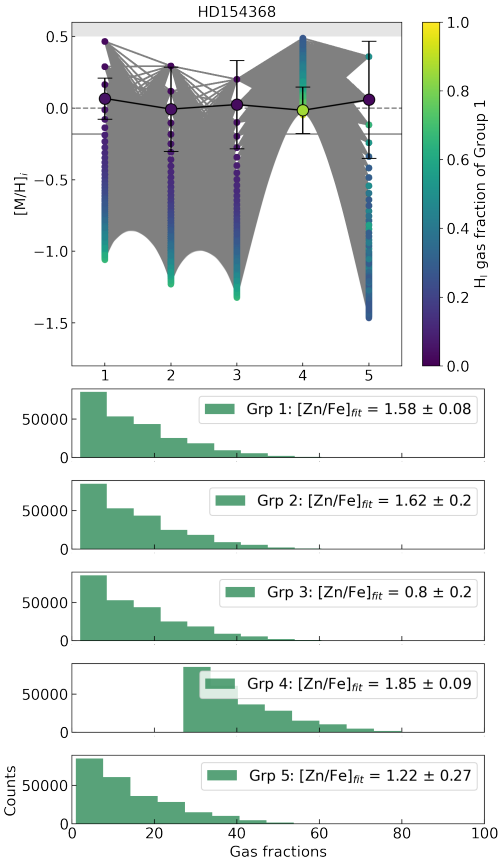

Fig. B.3: Updated simulated metallicities for HD 154368.

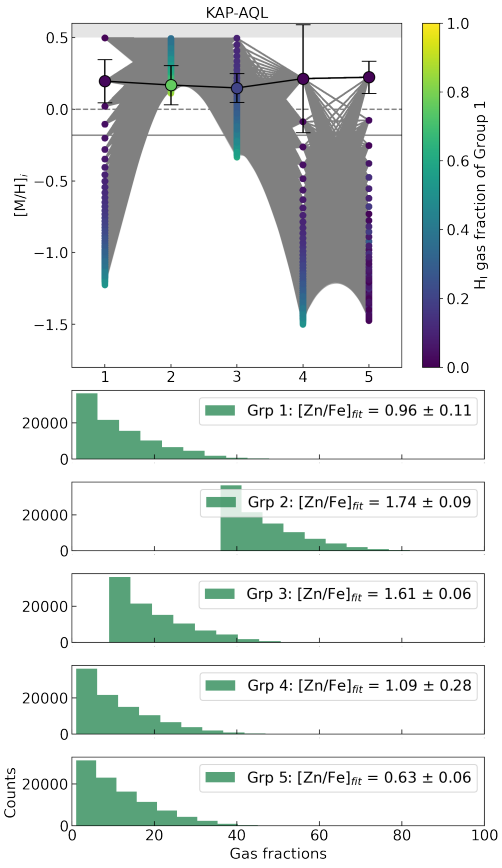

Fig. B.4: Updated simulated metallicities for κ Aql.

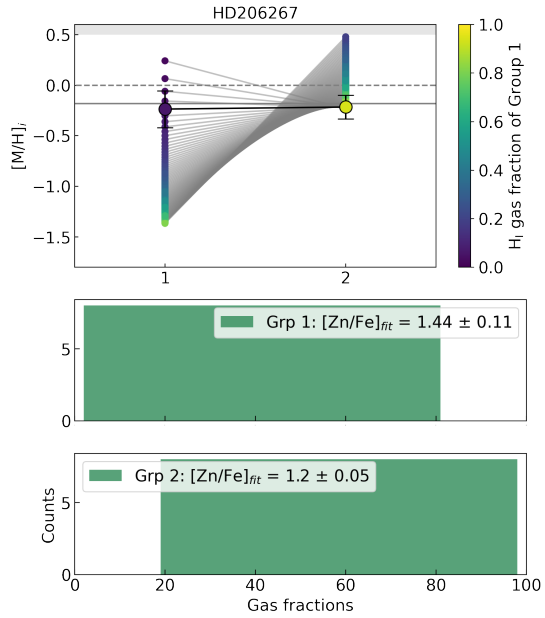

Fig. B.5: Updated simulated metallicities for HD 206267.

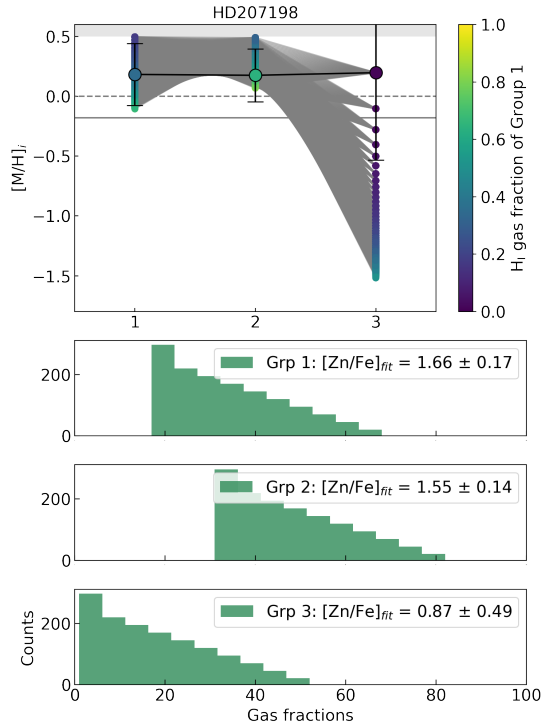

Fig. B.6: Updated simulated metallicities for HD 207198.

Appendix C: Updated comparison-to-literature plot

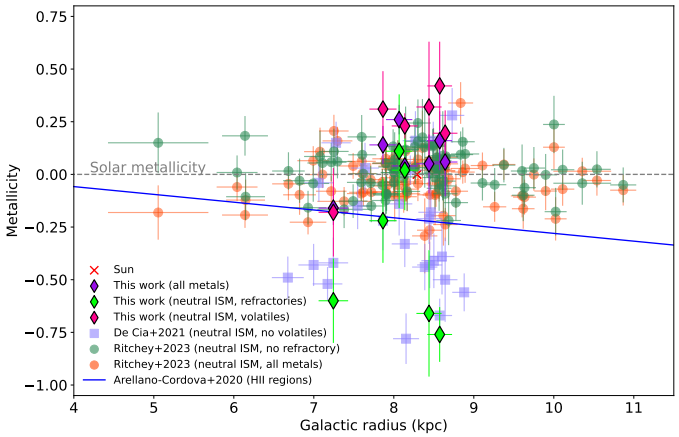

Fig. C.1: Updated comparison-to-literature plot for full lines of sight.